Mouse Folylpoly-γ-glutamate Synthetase Isoforms Respond Differently to Feedback Inhibition by Folylpolyglutamate Cofactors†

John L. Andreassi II and Richard G. Moran*

Department of Pharmacology and Toxicology and the Massey Cancer Center, Medical College of Virginia, Virginia Commonwealth University, Richmond, Virginia 23298

Received August 6, 2001; Revised Manuscript Received October 5, 2001

ABSTRACT: Folylpoly-γ-glutamate synthetase (FPGS) is the enzyme responsible for metabolic trapping of reduced folate cofactors in cells for use in nucleotide and amino acid biosynthesis. There are two isoforms of FPGS expressed in mouse tissues, one is expressed in differentiated tissue, principally liver and kidney, and the other in all rapidly proliferating cell types. The present study sought the functional difference that would explain the evolution of two mouse FPGS species. Recombinant cytosolic mouse isozymes were compared with respect to steady state kinetics, chain length of polyglutamate derivatives formed, and end-product inhibition by the major reduced folylpentaglutamate cofactors. Both isoforms were equally effective in catalyzing the addition of a mole of glutamic acid to reduced folate monoglutamate substrates. Each isoform was also capable of forming long chain polyglutamate derivatives of the model folate, 5,10-dideazatetrahydrofolate. In contrast, the FPGS isoform derived from rapidly proliferating tissue was much more sensitive to inhibition by (6*R*)-5,10-CH_2-H_4PteGlu$_5$ and (6*S*)-H_4PteGlu$_5$ than the isoform expressed in differentiated tissues, as demonstrated by 13- and 6-fold lower inhibition constants (K_i), respectively. Interestingly, each isozyme was equally sensitive to inhibition by (6*R*)-10-CHO-H_4PteGlu$_5$. We drew the conclusion that the decreased sensitivity of the FPGS expressed in mouse liver and kidney to feedback inhibition by 5,10-CH_2-H_4PteGlu$_{5-6}$ and H_4PteGlu$_{5-6}$ may have evolved to permit accumulation of a larger folate cofactor pool than that found within rapidly proliferating tissue.

5,6,7,8-Tetrahydrofolate (H_4PteGlu)[1] and its N5- and/or N10-substituted derivatives serve as donors and acceptors of one-carbon units in amino acid and nucleotide metabolism (*1*−*3*). In man and mouse, intracellular folates exist as tetrahydrofolylpoly-γ-glutamates with the penta- and hexaglutamate forms predominating (*3*, *4*). Tetrahydrofolylpoly-γ-glutamates represent the active folate coenzyme forms within mammalian cells (*5*), and these compounds serve as better cofactors for many of the folate-dependent enzymes than do the corresponding folylmonoglutamates (*6*). A single enzyme, folylpoly-γ-glutamate synthetase (FPGS, E.C. 6.3.2.17), metabolizes tetrahydrofolates to long chain polyglutamates (*7*) within the cytosol or mitochondria of mammalian cells (*8*). Addition of the polyglutamate side chain to tetrahydrofolate and its derivatives serves as a mechanism to trap these compounds within the cell (*9*): tetrahydrofolate derivatives containing less than three glutamates are not efficiently retained, and those containing four or more moles of glutamate per mole of pteridine are retained in most mammalian cells for extended periods of time (*8*). Thus, FPGS activity is crucial for the supply of reduced folate cofactors to the tetrahydrofolate-dependent enzymes in a form and at a concentration that efficiently drives the folate-dependent biosynthetic reactions.

Two species of cDNA for mouse FPGS have been isolated from cDNA libraries from mouse liver and leukemic (L1210) cells (*10*); the same two sequences have been isolated by 5′ RACE from these tissues (*11*). The cDNA species derived from each of these two tissues are identical in sequence over the region encoded by exons 2−15, but the mouse liver and L1210 sequences utilize alternate initial exons (*10*). As an additional level of heterogeneity, the initial exons utilized in the FPGS transcripts in both liver and dividing tissues contained two consensus translational start codons that are used for the production of mitochondrial and cytosolic forms of FPGS (*11*). Our laboratory (*11*) recently demonstrated that the mRNAs corresponding to the cDNA sequences found in mouse liver and L1210 cells exhibited a distinct pattern of distribution within tissues of the mouse. One variant is expressed predominantly in mouse liver and kidney, and the other is the only form found in proliferating tissues, both normal and neoplastic. Mouse liver and L1210 *fpgs* cDNA were shown to encode catalytically active FPGS protein in vivo and in vitro (*11*). Thus, expression plasmids containing each cDNA sequence were transfected into CHO-AUXB1 cells [a CHO-K derivative that is null function for FPGS

† Supported in part by Grants CA-39687 and CA-27605 from the National Institutes of Health, DHHS.

* To whom correspondence should be addressed: Medical College of Virginia, Virginia Commonwealth University, 1101 E. Marshall street, Richmond, VA 23298-0230. E-mail: rmoran@hsc.vcu.edu. Phone: (804) 828-9645. Fax: (804) 828-5782.

[1] Abbreviations: FPGS, folylpoly-γ-glutamate synthetase; 5′ RACE, 5′ rapid amplification of cDNA ends; DEAE, diethylaminoethyl; DDATHF, (6*R*)-5,10-dideaza-5,6,7,8-tetrahydrofolate; H_4PteGlu, 5,6,7,8-tetrahydropteroylglutamate; H_4PteGlu$_5$, 5,6,7,8-tetrahydropteroyl pentaglutamate; 2-ME, 2-mercaptoethanol; EDC, 1-ethyl-3(3-dimethylaminopropyl)carbodiimide-HCl; DTT, dithiothreitol; MOPS, 3-[*N*-morpholino]propanesulfonic acid; CM-sepharose, carboxymethylsepharose; SHMT, serine hydroxymethyltransferase.

10.1021/bi015644d CCC: $22.00
Published on Web 12/04/2001

```
   L.casei   1 MNYTETVAYI HSFPRLAKTG DHRRILTLLH ALGNPQQQGR  40
 H.sapiens   1 MEYQDAVRML NTLQTNAGYL EQVKRQRGDP QTQLEAMELY  40

M.musculus
     L1210   1 ME-------- -------YQD AVRTLNTLQT NASYLEQVKR  25
Mouse liver  1 MEWKDPSGSA YEAKTASFQD AVRTLNTLQT NASYLEQVKR  40
            41 QRSDPQAQLE AMEMYLARSG LQVEDLNRLN IIHVTGTKGK  80
            81 GSTCAFTERI LRNYGLKTGF FRSPHMVQVR DRIRINGKPI 120
           121 SPELFTKHFW CLYNQLEEFK DDSHVSMPSY FRFLTLMAFH 160
           161 VFLQEKVDLA VVEVGIGGAF DCTNIIRKPV VCGVSSLGID 200
           201 HTSLLGDTVE KIAWQKGGIF KPGVPAFTVV QPEGPLAVLR 240
           241 DRAQQIGCPL YLCPPLEALE EVGLPLSLGL EGAHQRSNAA 280
           281 LALQLAHCWL ERQDHQDIQE LKVSRPSIRW QLPLAPVFRP 320
           321 TPHMRRGLRD TVWPGRTQIL QRGPLTWYLD GAHTTSSVQA 360
           361 CVHWYRQSLE RSKRTDGGSE VHILLFNSTG DRDSAALLKL 400
           401 LQPCQFDYAV FCPNVTEVSS IGNADQQNFT VTLDQVLLRC 440
           441 LQHQQHWNGL AEKQASSNLW SSCGPDPAGP GSLLLAPHPP 480
           481 QPTRTSSLVF SCISHALLWI SQGRDPIFQP QSLPRNLLNH 520
           521 PTANSGASIL REAAAIHVLV TGSLHLVGGV LKLLDPSMSQ 560
```

FIGURE 1: Sequence comparison of *L. casei*, human and mouse FPGS. L1210 and mouse liver FPGS isoforms differ in amino terminal sequence (AA 1−19) but have identical sequences from Asp 20 onward. The underlined amino acids in the *L. casei* sequence correspond to an α-helix in the *L. casei* crystal structure (*12*). A fifteen residue gap (dashes) was introduced into the L1210 sequence to allow optimal alignment. Sequences were obtained from ref *11* and from the Swiss-Prot database.

and, thus, auxotrophic for thymidine, purines, and glycine (*7*, *9*)] and were shown to complement the auxotrophic phenotype of this cell (*11)*. In addition, mouse liver and L1210 cytosolic FPGS produced as purified, recombinant proteins were found to be functional by direct enzyme kinetics (*11*).

Cytosolic mouse liver and L1210 FPGS isozymes differ by 18 amino acids at their amino terminus (Figure 1). The amino terminal peptide in mammalian FPGS corresponds to a region of the *Lactobacillus casei* protein that has been shown to be an α-helix by X-ray crystallography (*12*). The amino terminal α-helix in the *L. casei* FPGS protein (PDB entries 1FGS and 1JBW) is intimately associated with the Ω loop, a highly conserved structural motif that makes up part of the active site (*13*, *14*). Thus, alterations in the amino-terminal structure of FPGS may influence the catalytic and/or substrate binding properties of this enzyme. However, our current understanding of FPGS based on the available structural and kinetic data do not explain why the mouse evolved two catalytically active, but different, species of this enzyme in tissues programmed for division or for differentiated function.

The present study was undertaken to elucidate the purpose of the two FPGS isoforms by more intensive investigation of the properties of recombinant cytosolic mouse liver and L1210 isozymes. We now report that the L1210 isoform is substantially more sensitive to feedback inhibition by long chain folylpolyglutamate cofactors than mouse liver FPGS. We have concluded from our results that inhibition of FPGS by cellular folylpolyglutamates represents a feedback mechanism for control of the size of the reduced folate cofactor pool and that the set point of this control system is different in dividing and nondividing tissues of the mouse.

MATERIALS AND METHODS

Reagents. All chemicals and reagents were purchased from Fisher Scientific (Fair Lawn, NJ) or Sigma Chemical Co. (St. Louis, MO) unless otherwise stated. Pteroylpentaglutamate, (6S)-5-CH_3-H_4PteGlu, and (6S)-5-CHO-H_4PteGlu were purchased from Schircks Laboratories (Jona, Switzerland); (6*R*)-10-CHO-H_4PteGlu was prepared as previously described (*15*). (6*S*)-5,6,7,8-H_4PteGlu was produced by enzymatic reduction and was purified by DEAE-cellulose chromatography as previously described (*16*) and was stored under N_2 at −20 °C. (6*R*)-5,10-dideaza-H_4PteGlu (DDATHF), (6*R*,*S*)-5,10-dideaza-H_4PteGlu$_{1-6}$, and 4-amino-PteGlu$_{2-3}$ (Aminopterin) were kindly provided by Dr. Chuan Shih of Eli Lilly Corporation, Indianapolis, IN. 3,4-^{3}H-L-glutamic acid (42 Ci/mmol) was purchased from ICN Biochemicals Inc. (Costa Mesa, CA). Tetrabutylammonium hydrogen sulfate (low UV Pic A) was purchased from Waters (Milford, MA), and ultrapure ammonium sulfate was purchased from ICN Biomedicals (Aurora, OH).

Production of Folylpentaglutamate Cofactors. The production of (6*S*)-5,6,7,8-H_4Pteglu$_5$ and the conversion of this compound to substituted pentaglutamate cofactors were monitored and quantitated by ultraviolet spectroscopy on a Hewlett-Packard 8453 UV−visible spectrophotometer, and spectra were analyzed with Chemstation software (Hewlett-Packard), based on extinction coefficients published for the various folylmonoglutamates (*17*). Pteroylpentaglutamate (14 μmol) was reduced to 7,8-H_2PteGlu$_5$ with NaS_2O_4 (*18*) using a ratio of 137 mol of NaS_2O_4/mol of PteGlu$_5$ (*19*) in the presence of 10% sodium ascorbate for 2.5 h at room temperature, protected from light. Product was purified twice by acid precipitation (*20*), lyophilized, and stored under N_2. H_2PteGlu$_5$ (4 μmol), at a final concentration of 0.2 mM, was enzymatically reduced at 37 °C with 5 units of *L. casei* DHFR in 25 mM KPO_4 buffer (pH 7.5), in the presence of 1 mM NADPH and 20 mM 2-mercaptoethanol (2-ME) (*16*, *21)*. When the absorbance at 340 reached a minimum, the DHFR reaction was quenched on ice, made 0.2 M in 2-ME, and applied to a 0.9 × 35 cm DEAE-Sephacel column equilibrated in 50 mM ammonium acetate buffer, pH 7.0, containing 1% 2-ME. (6*S*)-H_4PteGlu$_5$ was eluted with a 190 mL linear gradient of 0.05−1.5 M ammonium acetate containing 1% 2-ME. (6*S*)-H_4PteGlu$_5$ intended for use in producing (6*S*)-5-CHO-H_4PteGlu$_5$ was purified by similar chromatography using ammonium formate as the elution buffer. (6*R*)-5,10-CH_2-H_4PteGlu$_5$ was made immediately before use by incubation of column-purified (6*S*)-H_4PteGlu$_5$ with a solution (pH 4.5) containing 40 mM formaldehyde (*17*), and the product was used in kinetic experiments within an hour without further purification. The final concentration of formaldehyde in all FPGS reactions containing (6*R*)-5,10-CH_2-H_4PteGlu$_5$ was adjusted to 2 mM. (6*S*)-5-CH_3-H_4-PteGlu$_5$ was produced by chemical reduction of (6*R*)-5,10-CH_2-H_4PteGlu$_5$ with $NaBH_4$ (*22*). Briefly, (6*S*)-H_4PteGlu$_5$ (3 μmol) was dissolved in degassed 250 mM $NaPO_4$ buffer (pH 7.5) containing 300 mM formaldehyde in a final volume of 200 μL. $NaBH_4$ (4 mg) was added, and reactions were incubated at 37 °C for 1 h under a steady stream of N_2. After incubation, the reaction mixture was made 100 mM in 2-ME, and the pH was adjusted to 7.5 with 5 N acetic acid; the volume was brought to 1 mL with 1% 2-ME, and the solution was applied to a 0.9 × 35 cm DEAE-Sephacel column equilibrated in 50 mM ammonium acetate (pH 7.0) containing 1% 2-ME. (6*S*)-5-CH_3-H_4PteGlu$_5$ was eluted with a 460 mL, convex gradient of 0.05−1.5 M ammonium acetate containing 1% 2-ME. (6*S*)-5-CHO-H_4PteGlu$_5$ was synthesized via activation of excess formic acid with 1-ethyl-3(3-dimethylaminopropyl) carbodiimide-HCl and subsequent

formylation of (6*S*)-H_4PteGlu$_5$, followed by chromatographic purification as previously described (*23*). (6*R*)-10-CHO-H_4PteGlu$_5$ was produced from (6*S*)-5-CHO-H_4PteGlu$_5$ via isomerization by acidic then basic pH shifts (*15*) and was purified by HPLC on a 100 × 4.6 mm, 5 μm, Luna C_{18} reverse phase column (Phenomenex, Torrance, CA) using isocratic elution with 37.5% methanol and 62.5% Pic A (final pH = 7.8). All HPLC buffers were rigorously degassed by vacuum, and then by purging with helium during chromatography. (6*R*)-10-CHO−H_4PteGlu$_5$ was the major peak with retention time ≈ 10 min and was identified by its UV spectrum. To remove the methanol and PicA reagent, the (6*R*)-10-CHO-H_4PteGlu$_5$ peak (≈1.5 mL) was combined with 7 μL of 2-ME and 100 μL of a slurry of DEAE-Sephacel equilibrated with 2 mM ammonium acetate (pH 7.0) and 50 mM 2-ME (buffer A), and the mixture was rotated at 4 °C for 15 min. The resin was washed once with buffer A, resuspended in this buffer, and transferred to a 0.22 μ Costar Spin-X filter (Corning Inc., Corning, NY). The wash buffer was removed by centrifugation without drying the resin, and (6*R*)-10-CHO-H_4PteGlu$_5$ was immediately eluted with 200 μL of 2 M ammonium acetate containing 50 mM 2-ME. The purified (6*R*)-10-CHO-H_4PteGlu$_5$ was quantitated by spectrophotometry (λ_{max} = 260 nm, ϵ = 17 mM^{-1} at pH 7.5)[2] and immediately used in kinetic experiments.

Production and Purification of Recombinant Mouse Liver and L1210 FPGS. The construction of recombinant baculoviruses allowing expression of mouse liver and L1210 FPGS was previously described (*11*). Purification of mouse liver and L1210 FPGS employed a slight modification of the procedure used for recombinant human cytosolic FPGS (*24*). Cultures of SF9 cells (800 mL at 2 × 10^6 cells/mL) were infected with baculovirus expressing either mouse liver or L1210 FPGS at an MOI of 1.2. After a 60 h incubation at 27 °C, SF9 cells were harvested by centrifugation, resuspended in 60 mL of cell lysis buffer [100 mM Tris, pH 7.9 (at 25 °C), 2 mM dithiothreitol (DTT), 2 mM ATP, 5 mM $MgCl_2$, 0.05% *n*-octylglucoside, and complete protease inhibitor cocktail tablets (Boehringer Mannheim, Germany) at a 2× final concentration], and sonicated. The lysates were centrifuged at 110000*g* for 1 h, and the supernatant was purified via a sequential three-step process consisting of 36% $(NH_4)_2SO_4$ precipitation, gel filtration chromatography on a Sephacryl HR 200 (Amersham Pharmacia Biotech) column and ion-exchange chromatography on a DEAE-Sephacel column (*24*). Peak fractions of DEAE-Sephacel purified FPGS protein were pooled, concentrated, and stored in 50% glycerol at −20 °C. The elution positions of mouse liver and L1210 FPGS after gel filtration and ion exchange chromatography were similar with those seen with the human enzyme (*24*). Additional purification of L1210 FPGS was performed by cation-exchange chromatography on a 0.9 × 30 cm CM-Sepharose column (Amersham Pharmacia Biotech). This column was equilibrated in buffer A (20 mM, 3-[*N*-morpholino]propanesulfonic acid (MOPS), pH 7.3 at 4 °C and 1 mM DTT), and L1210 FPGS was applied to the column in buffer A. The column was washed with two column volumes of buffer B [20 mM MOPS (7.3), 1 mM DTT, and 20 mM KCl], and enzyme was eluted with a 100 mL linear gradient of 20−350 mM KCl in buffer B, at a flow rate of 1 mL/min; 2.5 min fractions were collected. Peak fractions were pooled, concentrated, and stored in 50% glycerol. Protein was determined by a dye binding based assay (*25*) (Bio-Rad Laboratories, Hercules, CA).

Steady-State Kinetic Analysis of Mouse Liver and L1210 FPGS Isoforms with Monoglutamate Antifolates and Reduced Folate Cofactors. Standard reactions were conducted in duplicate for 1 h at 37 °C in a total volume of 250 μL containing: 3.5 nM mouse liver or L1210 FPGS, 0.2 M Tris (pH 8.9 at 25 °C), 30 mM KCl, 10 mM $MgCl_2$, 1 mM ^{3}H-L-glutamic acid (4.0 mCi/mmol), 5 mM ATP, 50 mM 2-ME, and 0.3 mg/mL bovine serum albumin. Enzyme reaction conditions were varied such that less than 15% of the monoglutamate substrate was consumed at any concentration so that the measured rates should reflect formation of diglutamate product. For extremely efficient substrates ((6*S*)-H_4PteGlu and (6*R*)-10-CHO-H_4PteGlu), reaction volumes of 1 mL were necessary to limit consumption to less than 15%. Reaction products were quantitated via charcoal adsorption as described previously (26). Saturation curves were fitted to a rectangular hyperbola using Enzfitter software (Elsevier Biosoft) to derive values for K_m and k_{cat}. Kinetic behavior of each folate/antifolate monoglutamate substrate was determined for both mouse liver and L1210 FPGS in the same assay; kinetic constants represent the average of at least three experiments (except when noted), performed on separate days. Reduced compounds such as (6*S*)-H_4PteGlu and (6*S*)-5-CH_3-H_4PteGlu were stored as dry powder under N_2 and made into stock solutions containing 2-ME (1%), immediately prior to assay.

Determination of K_i Values for Folylpentaglutamate Cofactors and DDATHF Pentaglutamate. For (6*S*)-H_4PteGlu$_5$, (6*R*)-5,10-CH_2-H_4PteGlu$_5$, and (6*R*)-10-CHO-H_4PteGlu$_5$, FPGS inhibition experiments were composed of three saturation curves each at a different fixed folylpentaglutamate concentration. Aminopterin at concentrations ranging from 0 to 25 × K_m was utilized as the variable substrate. Reaction conditions were identical to those described above for kinetic analysis of monoglutamate cofactors except that reactions were preincubated for 5 min at 37 °C with folylpentaglutamate, and then reactions were initiated with increasing amounts of aminopterin. Reaction rates of mouse liver or L1210 enzyme incubated with folylpentaglutamate alone were the same as background. Hence, under these assay conditions, the addition of glutamic acid to folylpentaglutamate did not contribute to the reaction rate observed for either L1210 or mouse liver FPGS. Reaction velocities were transformed via a double reciprocal plot, and linear regression with data weighted proportionally to v^4 (*27*), generated in SigmaPlot (Jandel Scientific), was used to fit the data. Linear replots of reciprocal slope and reciprocal V_{max} were used to calculate values for $K_{i,slope}$ and $K_{i,Vmax}$. Data were also analyzed by nonlinear curve fit and gave identical results. For 5-CHO-H_4PteGlu$_5$ and 5-CH_3-H_4PteGlu$_5$, which inhibited FPGS only at high concentrations, inhibition was analyzed by Dixon plots with 45 μM aminopterin as the fixed substrate. Inhibition studies with DDATHF pentaglutamate used 30 μM aminopterin as the fixed substrate. In the Dixon experiments, FPGS isozymes were preincubated with inhibitor for 5 min at 37 °C, and reactions were initiated by addition of a constant amount of aminopterin. Velocity data were analyzed via plots of reciprocal velocity verses [I] and

[2] Personal communication, Professor Verne Schirch.

Table 1: Kinetic Parameters of Substrates for Recombinant Mouse Liver and L1210 FPGS[a]

	K_m (μM)	k_{cat} (min^{-1})	k_{cat} relative to H_4PteGlu	k_{cat}/K_m (M^{-1} min^{-1}) × 10^6
		mouse liver		
aminopterin	17.7 ± 4.0	13.2 ± 1.5	1.02	0.78 ± 0.2
(6*R*)-DDATHF	7.6 (0.75)	8.7 (1.8)	0.67	1.2 (0.34)
(6*S*)-H_4PteGlu	6.3 ± 4.0	12.9 ± 3.0	1.0	2.9 ± 1.9
(6*R*)-10-CHO-H_4PteGlu	2.9 ± 0.02	12.7 ± 1.2	0.98	4.4 ± 0.43
(6*S*)-5-CH_3-H_4PteGlu	64± 6.0	13.2 ± 1.4	1.02	0.21 ± 0.002
(6*S*)-5-CHO-H_4PteGlu	122 ± 2.8	6.9 ± 0.07	0.53	0.057 ± 0.0021
		L1210		
aminopterin	15.4 ± 2.9	9.9 ± 0.98	1.4	0.66 ± 0.15
(6*R*)-DDATHF	1.2 (0.23)	0.62 (0.005)	0.09	0.55 (0.11)
(6*S*)-H_4PteGlu	1.4 ± 0.04	7.0 ± 2.0	1.0	5.1 ± 1.8
(6*R*)-10-CHO-H_4PteGlu	2.0 ± 0.04	5.7 ± 0.7	0.8	2.8 ± 0.42
(6*S*)-5-CH_3-H_4PteGlu	54 ± 1.0	6.7 ± 0.7	0.95	0.12 ± 0.011
(6*S*)-5-CHO-H_4PteGlu	75 ± 1.1	4.4 ± 0.2	0.6	0.059 ± 0.0014

[a] Values are the mean ± SD of ≥3 experiments (two in the case of DDATHF, where values are the mean with the one-half the range shown in parentheses) performed on different days.

K_i values were calculated using the Dixon equation for competitive inhibition. Each K_i value represents the mean of two experiments performed on separate days.

In Vitro Polyglutamation of DDATHF and Aminopterin by Mouse Liver and L1210 FPGS. The ability of mouse liver and L1210 FPGS to form long chain polyglutamate products of DDATHF and aminopterin was determined by HPLC. FPGS (0.08 μM) was incubated at 37 °C in a total volume of 0.5 mL with 10 μM DDATHF or 40 μM aminopterin and 5 mM ^{3}H-L-glutamic acid (8 μCi/μmol). Reactions were terminated at 100 °C for 2 min, brought to 1 mL with double-strength Pic A (pH 6.0), and centrifuged at 14 000 rpm to remove precipitated protein. Unincorporated ^{3}H-L-glutamic acid was removed with Sep-Pak C_{18} cartridges (Waters Corp.) (28). Products eluted from Sep-Pak columns were dried, resupended in 400 μL Pic A, and passed through a 0.22 μ Costar SPIN-X filter; 100 μL of each reaction was injected onto a 100 × 4.6 mm, 3 μm, Luna C_{18} reverse phase column. DDATHF polyglutamates were separated with an 0.8 mL/min multiphasic gradient of methanol and Pic A (pH = 6.0): a mobile phase of 36% methanol was held constant for 5 min, then increased to 44% over 10 min, further increased to 45.6% over 15 min, and finally brought to 46.4% by 36 min. Aminopterin polyglutamates were also separated with a gradient of methanol and Pic A (pH = 6.0): methanol was held constant at 29.6% for the first 3 min, increased to 38.4% methanol over 15 min, then increased to 39.2% over 3.3 min, further increased to 42.4% over 14 min, and finally brought to 50.4% by 40.3 min. Elutants were monitored at 280 nm and 0.5 min fractions were collected. Fractions were analyzed by scintillation counting. Chain lengths of DDATHF and aminopterin polyglutamates were identified by comparison of the retention times of known standards.

RESULTS

Production and Purification of Mouse FPGS Isozymes. Mouse liver FPGS was expressed from a recombinant baculovirus and purified from infected Sf9 cells using a three-step procedure consisting of $(NH_4)_2SO_4$ precipitation, gel filtration on Sephacryl HR 200, and DEAE-Sephacel chromatography, as previously optimized for human FPGS (*24*). The *fpgs* cDNA cloned from mouse L1210 cells was, likewise, expressed from a baculoviral construct, and the encoded protein was purified by the same technique as used for the mouse liver enzyme, but was then further purified by chromatography on a column of CM-Sepharose. These purification procedures brought both isoforms of mouse FPGS to a purity greater than 95% as judged by SDS−PAGE (Figure 2). The mouse liver and L1210 FPGS species had molecular masses of 62 and 60.6 kDa, respectively, as calculated from their predicted amino acid sequences (Figure 1). From an 800 mL culture of insect cells, 4−6 mg of purified protein was obtained, with a yield of 20% based on enzyme levels in crude cell sonicates. Both enzymes were quite stable when stored at −20 °C in buffered 50% glycerol, and purified enzymes (Figure 2) were used for all experiments discussed in this report.

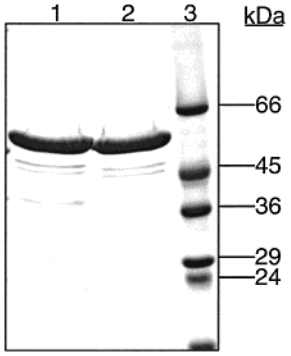

FIGURE 2: Purity of recombinant mouse liver and L1210 FPGS. Mouse liver (lane 1) or L1210 (lane 2) FPGS (5 μg) was applied to a 10% SDS−PAGE gel which was stained with Coomassie Blue after electrophoresis. Lane 3 contains molecular mass markers with sizes shown in kDa.

Steady-State Kinetics. The kinetics with which mouse liver and leukemic cell FPGS utilized several tetrahydrofolate cofactor forms and two central folate antimetabolites was studied by steady-state methods. This kinetic analysis revealed some consistent differences in substrate preference between the two mouse isoforms, but the two proteins were much more similar than they were different (Table 1). (6*S*)-H_4PteGlu and (6*R*)-10-CHO-H_4PteGlu were the best naturally occurring substrates for both enzymes, as judged by high k_{cat} values, low K_m values, and high second-order rate constants (k_{cat}/K_m). The average turnover number for the mouse liver FPGS using 5-CH_3-H_4PteGlu, 10-CHO-H_4-PteGlu, and H_4PteGlu as substrates was 12.9 min^{-1}, about double that of the mouse L1210 FPGS (6.5 min^{-1}). However,

the second-order rate constants for H_4PteGlu and 10-CHO-H_4PteGlu were nearly identical for the two mouse isoforms. The data suggest that in all mouse tissues, H_4PteGlu and 10-CHO-H_4PteGlu are the folylmonoglutamate forms that are most easily converted to higher glutamate derivatives. (6*S*)-5-CHO-H_4PteGlu and (6*S*)-5-CH_3-H_4PteGlu had substantially higher K_m values than the other tetrahydrofolates and (6*S*)-5-CHO-H_4PteGlu also had a lower k_{cat} for both mouse isozymes. Hence, we conclude that both are poor substrates and that 5-CHO-H_4PteGlu, in particular, is unlikely to be converted to higher glutamate forms in vivo without initial conversion to other folate derivatives. The poor substrate activity of 5-CHO-H_4PteGlu for both of these pure mouse FPGS species agrees with prior studies on pure human enzyme (*29*) and indicates that the previously reported higher activity of 5-CHO-H_4PteGlu for partially purified mouse liver FPGS (*30*) was the result of contaminating isomerases. Fromm (*31*) has reasoned that the second-order rate constants for an ordered sequential kinetic mechanism constitute on rates for substrates; such a mechanism has been demonstrated for hog liver FPGS by Shane and his colleagues using aminopterin as a substrate (*32*). Hence, these data would suggest that the rate of binding of 5-CHO-H_4PteGlu to the surface of mouse liver or L1210 FPGS was 50−80 times slower than that of H_4PteGlu and 10-CHO-H_4PteGlu, and also that 5-substituted tetrahydrofolates, in general, adsorb to an FPGS active site binding surface slowly.

The kinetic patterns observed with the two antifolates DDATHF and aminopterin were the most divergent with the two enzymes in this series of substrates. Aminopterin had near identical kinetic characteristics with the two FPGS isoforms. DDATHF, on the other hand, showed the largest difference in kinetics with the two mouse FPGS species. The K_m of mouse liver FPGS for DDATHF was 6-fold higher than that for the L1210 cell enzyme, but the L1210 isozyme had a much lower k_{cat} (14-fold) with DDATHF as a substrate than did the mouse liver enzyme. Although the kinetics of the two mouse FPGS isozymes were distinguishable, they did not give any insight into why the mouse made two species of FPGS.

In Vitro Formation of Folylpolyglutamates by the Mouse FPGS Isoforms. A single species of pure human FPGS has been shown to allow the formation of folate polyglutamates with long side chains in vitro with some but not all substrates. To determine whether the two mouse FPGS species differed in the ability to extend the side chain beyond a single addition, each pure enzyme was incubated with saturating amounts of glutamic acid and ATP and the antifolates DDATHF or aminopterin. (In our previous experience, DDATHF was one of the substrates most rapidly promoted to long chain polyglutamates by recombinant human FPGS (*24*) whereas aminopterin is largely converted only to the diglutamate). Analysis of reaction products by HPLC from incubations with 0.08 μM mouse liver or L1210 FPGS indicated that both enzymes converted DDATHF to long chain polyglutamate derivatives. Although there were clear differences in the rate of polyglutamation at 10 μM DDATHF, which were expected based on the kinetic characteristics of the two enzymes (Table 1), the two mouse enzymes converted DDATHF to penta- and hexaglutamate derivatives with no appreciable accumulation of the diglutamate homologue (Figure 3B−E). On the other hand, incubation of either

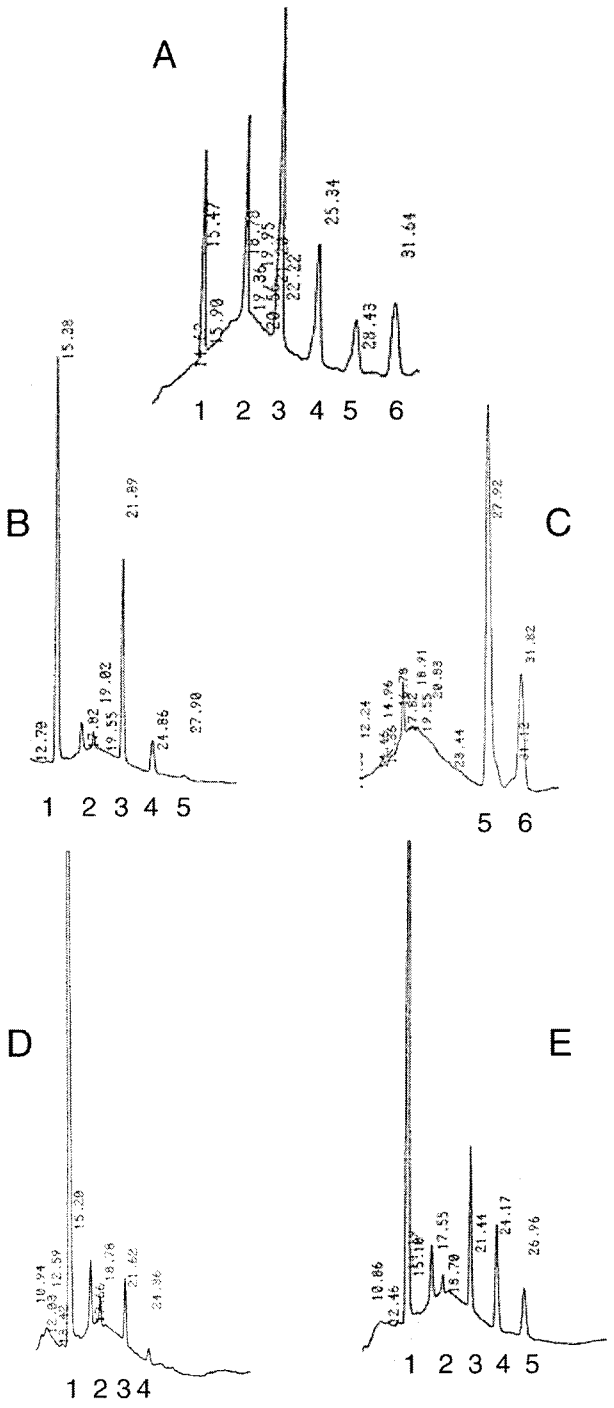

FIGURE 3: Separation of mouse liver and L1210 FPGS reaction products by reversed-phase HPLC. (A) The elution position of DDATHF mono- and polyglutamate standards are denoted as 1−6, with 1 representing the monoglutamate. Mouse liver FPGS was incubated with 10 μM DDATHF for 10 min (B) or 120 min (C). L1210 FPGS was incubated with 10 μM DDATHF for 10 min (D) or 120 min (E).

enzyme with 40 μM aminopterin resulted in rapid and near quantitative conversion of aminopterin to the diglutamate derivative, but conversion of the diglutamate of aminopterin to triglutamate was quite slow with either enzyme (data not shown). Hence, there was no significant difference in the ability of the two mouse FPGS isoforms to convert DDATHF or aminopterin to polyglutamates.

Inhibition of Mouse Liver and L1210 FPGS by DDATHF Pentaglutamate. Polyglutamates of tetrahydrofolate have

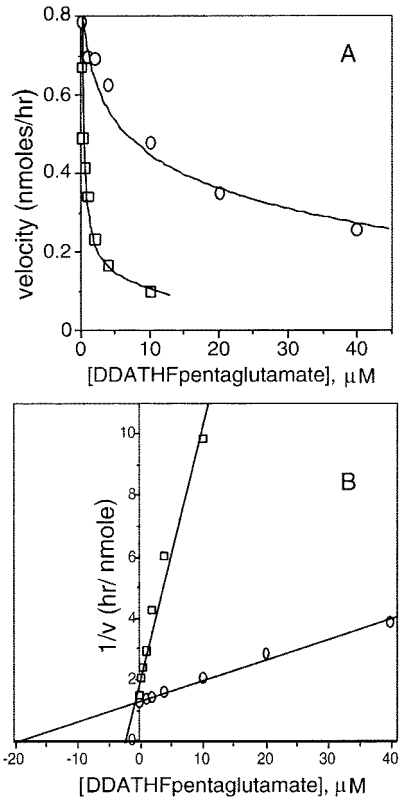

FIGURE 4: Inhibition of mouse liver (O) and L1210 (□) FPGS by DDATHF pentaglutamate. (A) Velocity of mouse liver and L1210 FPGS as a function of DDATHF pentaglutamate concentration. (B) Subsequent Dixon analysis of inhibition of mouse FPGS by DDATHF pentaglutamate.

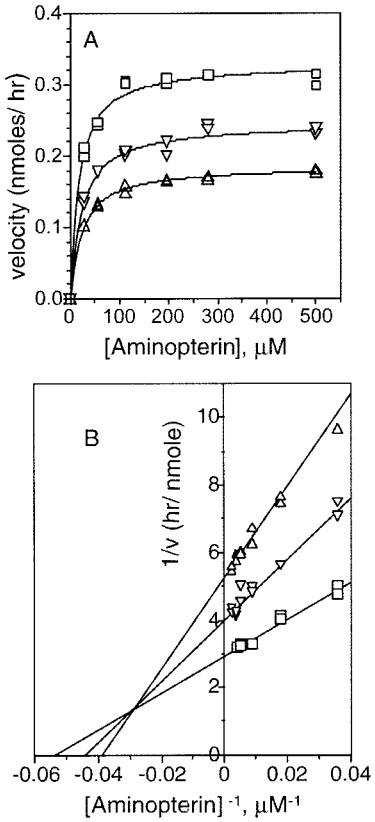

FIGURE 5: Kinetics of inhibition of L1210 FPGS by 10-CHO-H_4-$PteGlu_5$. (A) L1210 FPGS was incubated with the indicated concentrations of aminopterin in the presence of 0 (□), 1 μM (∇), or 3 μM (Δ) 10-CHO-$H_4PteGlu_5$. (B) Transformation of the data in panel A and subsequent weighted linear regression demonstrates the mixed-type pattern of inhibition typical for folylpentaglutamate cofactors.

been shown to bind to mammalian FPGS with K_m values on the range of 2−3 μM, but the reaction proceeds only with a very low velocity using these compounds as substrates (*32*). Hence, folylpolyglutamates are potential inhibitors of FPGS. A previous study has shown that the conversion of DDATHF to polyglutamates in leukemic cells was limited by an expanded cellular folate pool (*33*), the first reported evidence of which we are aware for the operation of feedback control in this pathway in vivo. Hence, the sensitivity of mouse liver and mouse leukemic cell FPGS to inhibition by a stable, pure long-chain folate analogue, DDATHF pentaglutamate, was studied. As shown in Figure 4A, both enzyme isoforms were inhibited by the pentaglutamate derivative of DDATHF, but the L1210 form of FPGS was inhibited to a greater extent at lower concentrations of compound than was the mouse liver enzyme. When this inhibition was subjected to Dixon analysis (Figure 4B) assuming that the binding of inhibitor (DDATHF pentaglutamate) and substrate (aminopterin) were mutually exclusive, the K_i values estimated for mouse liver FPGS (7.4 μM) and L1210 FPGS (0.83 μM) differed by a factor of 9.

Kinetics of Inhibition of Mouse FPGS Isoforms by Cellular Folate Cofactor Polyglutamates. It became of interest to determine whether the difference in sensitivity of mouse liver and L1210 FPGS to inhibition by DDATHF pentaglutamate was specific for this compound or whether it extended to the polyglutamate folate cofactor forms found in mammalian cells. Hence, the pentaglutamate form of each of the major reduced folate cofactors was prepared, purified, and studied as inhibitors of both mouse FPGS species. The results of a representative experiment, in which (6*R*)-10-CHO-$H_4PteGlu_5$ was used as an inhibitor and aminopterin was used as a substrate, are shown in Figure 5. Reactions performed in the absence of aminopterin were included in each experiment and did not demonstrate measurable formation of product from any of the pentaglutamate cofactors used in these studies. Concentrations of the substrate aminopterin as high as 25× K_m only partially reversed inhibition by (6*R*)-10-CHO-$H_4PteGlu_5$ (Figure 5A), and subsequent analyses of the data by either Lineweaver−Burk or Hofstee plots demonstrated that the inhibition had both competitive and noncompetitive components (Figure 5B). The mixed inhibition pattern shown in Figure 5B was observed for both mouse liver and L1210 FPGS with all of the substrates [(6*S*)-H_4-$PteGlu_5$, (6*R*)-10-CHO-$H_4PteGlu_5$, and (6*R*)-5,10-CH_2-H_4-$PteGlu_5$] for which inhibition was potent enough to allow this experimental design with the quantities of tetrahydrofolylpentaglutamates available. For these inhibitors, both reciprocal slope and reciprocal intercept replots were linear with inhibitor concentration, giving individual estimates of the competitive and noncompetitive components of the inhibition pattern (Table 2). The kinetics of inhibition of both L1210 and mouse liver FPGS by (6*R*)-10-CHO-$H_4PteGlu_5$ were almost identical, and this compound proved to be a potent inhibitor of both enzymes. On the other hand, (6*S*)-$H_4PteGlu_5$, and (6*R*)-5,10-CH_2-$H_4PteGlu_5$ were potent inhibitors of L1210 FPGS but much poorer inhibitors of mouse liver FPGS. For (6*S*)-$H_4PteGlu_5$, (6*R*)-10-CHO-$H_4PteGlu_5$,

Table 2: Inhibition Constants of Tetrahydrofolylpentaglutamate Cofactors for Mouse Liver and L1210 FPGS[a]

	mouse liver		L1210	
	K_i slope (μM)	K_i intercept (μM)	K_i slope (μM)	K_i intercept (μM)
(6*S*)-$H_4PteGlu_5$	21 (4.0)	54 (10)	3.7 (0.25)	8.3 (1.8)
(6*R*)-5,10-CH_2-$H_4PteGlu_5$	22 (1.0)	43 (0.0)	1.7 (0.5)	8.3 (1.5)
(6*R*)-10-CHO-$H_4PteGlu_5$	2.4 (1.1)	5.2 (2.3)	2.3 (0.1)	4.2 (0.15)
(6*S*)-5-CH_3-$H_4PteGlu_5$	55 (2.5)	NA[b]	20 (0.0)	NA[b]
(6*S*)-5-CHO-$H_4PteGlu_5$	84 (22)	NA[b]	66 (15)	NA[b]

[a] Values represent the mean of two Lineweaver−Burk experiments; one-half the range is shown in parentheses. [b] NA, estimation of the competitive and noncompetitive inhibitor components for (6*S*)-5-CHO and (6*S*)-5-CH_3-$H_4PteGlu_5$ was not allowed by the experimental design compatible with the quantities of these compounds available.

and (6*R*)-5,10-CH_2-$H_4PteGlu_5$, the K_i values for the competitive component of this interaction was 2−2.5 times lower than the noncompetitive component. 5-CH_3-$H_4PteGlu_5$ was a relatively weak inhibitor of either mouse liver or L1210 FPGS. The K_i for 5-CH_3-$H_4PteGlu_5$ with the L1210 enzyme was, on the average, 8 times higher than for (6*S*)-$H_4PteGlu_5$, (6*R*)-10-CHO-$H_4PteGlu_5$, and (6*R*)-5,10-CH_2-$H_4PteGlu_5$, and the K_i for 5-CH_3-$H_4PteGlu_5$ for the mouse liver enzyme was 23 times higher than for (6*R*)-10-CHO-$H_4PteGlu_5$. Finally, 5-CHO-$H_4PteGlu_5$ was an equally poor inhibitor of both isozymes, with K_i values in the range of 65−85 μM. Hence, there was a near-qualitative difference in the level of inhibition of the mouse liver and L1210 cell FPGS by cellular polyglutamate cofactors. The most distinctive difference between the two mouse FPGS isoforms was that mouse liver FPGS was virtually unaffected by $H_4PteGlu_5$ and 5,10-CH_2-$H_4PteGlu_5$ at concentrations that substantially inhibited the activity of the L1210 isozyme. However, both enzymes were equally sensitive to polyglutamates of 10-CHO-H_4-PteGlu.

DISCUSSION

The mouse produces two isoforms of cytosolic FPGS, one of which is expressed in all proliferating cell types, and the other is expressed in liver and kidney. In this paper, we attempted to determine why two FPGS isoforms are made, that is, what difference in enzymatic function was so important that it drove evolution of the expression of two isozymes in this species, in such a strict tissue-dependent fashion. Steady-state kinetic analysis of mouse liver and L1210 FPGS demonstrated that the two isoforms were quite similar in catalyzing the addition of glutamic acid to the naturally occurring tetrahydrofolylmonoglutamate cofactors. Likewise, both FPGS species metabolized a model folate substrate to long chain polyglutamates that would be effectively retained by mammalian cells. With the L1210 cell FPGS, the in vitro polyglutamation reaction using DDATHF appears to be processive, suggesting that the folyl oligoglutamate product was not released between additions of glutamic acid, whereas the reaction with aminopterin demonstrated the opposite extreme behavior, compatible with requisite release of product before the next ligation reaction. Mouse liver FPGS showed exactly the same behavior. Hence, the catalytic behavior of the two active sites was strikingly similar. In contrast, the different response of mouse liver and L1210 FPGS to inhibition by tetrahydrofolylpentaglutamate cofactors functionally distinguishes these two enzymes. Polyglutamate substrates have previously been shown to be substrates for, and, hence, to bind to FPGS (*32*, *34*). In one particularly germane study, the k_{cat} of $H_4PteGlu_{1-7}$ was demonstrated to decrease drastically as the side chain length increases (*32*). Therefore, the long chain tetrahydrofolylpolyglutamate substrates, which comprise over 95% of intracellular folates in mammals (5, *32*), might act as inhibitors of the FPGS reaction. The physiological relevance of this inhibition has been uncertain, and others have debated the significance of the effect (*34*, *35*). On the basis of our new findings, we propose that this inhibition is operative as a feedback control on folate cofactor pool size and that the set point of this control mechanism differs in differentiated and dividing cell types in the mouse.

The difference between mouse liver and L1210 FPGS in sensitivity to inhibition by tetrahydrofolylpolyglutamates was most striking for $H_4PteGlu_5$ and 5,10-CH_2-$H_4PteGlu_5$ and to a lesser extent with 5-CH_3-$H_4PteGlu_5$, whereas both isoforms were equally inhibited by 10-CHO-$H_4PteGlu_5$. Hence, the binding of tetrahydrofolylpolyglutamates causative of the inhibition of the mouse FPGS species is heavily influenced by the orientation and binding of the tetrahydropteridine ring to the protein, most likely to the folate binding site in the active site, which in turn is modified by the amino terminal peptide of the FPGS species. The slow on rates (k_{cat}/K_m) for 5-CHO-H_4PteGlu and 5-CH_3-H_4PteGlu suggest that a substitution at the N-5 position of the pteridine interfered with binding to the folate pocket in the active site of both liver and L1210 FPGS, and 5-CH_3-$H_4PteGlu_5$ and 5-CHO-H_4-$PteGlu_5$ are poor inhibitors of both enzymes. Likewise, the feedback inhibition of $H_4PteGlu_5$ is much more pronounced for the L1210 FPGS than for mouse liver FPGS, and the K_m values for H_4PteGlu differ by a factor of 4.5. Finally, the kinetic constants for utilization of 10-CHO-H_4PteGlu as a substrate are identical for the two mouse FPGS species as are the potencies of 10-CHO-$H_4PteGlu_5$ as a feedback inhibitor. Taken together, these observations strongly support the concept that the position of binding of the tetrahydropteridine ring of the folates for both catalysis and feedback inhibition is the same.

The only difference in the two mouse FPGS species is that the liver FPGS sequence contains an 18-residue amino terminal peptide not found in the L1210 enzyme (Figure 1). The three-dimensional structure of mammalian FPGS is not currently available so that we do not yet know how the amino terminal peptide affects the FPGS active site. However, in the structure of the *L. casei* FPGS, the amino terminal α-helix is in contact with the adjacent Ω loop (*12*), which positions the folate substrate in the active site (*14*). A role for the amino-terminal peptide in modifying the active site is also supported by mutagenesis experiments. Thus, a tyrosine at position 3 and an aspartate or glutamate at position 5 of cytosolic FPGS is highly conserved (Figure 1). A recent

Table 3: (A) Literature Estimates of Folate Cofactor Concentrations in Mouse Liver and L1210 Cells

(A) Tissue Concentrations of $H_4PteGlu_n$, 5,10-CH_2-$H_4PteGlu_n$, 5-CH_3-$H_4PteGlu_n$, and Total Folates

	mouse liver[a]				L1210[b]			
	cytosol[c] [μM]	K_i's[e]	mitochondria[c] [μM]	K_i's[e]	cytosol[d] [μM]	K_i's[e]	mitochondria[d] [μM]	K_i's[e]
$H_4PteGlu_{5-6}$ + 5,10-CH_2-$H_4PteGlu_{5-6}$	12−17	0.6−0.8	24−30	1.1−1.4	6.0	2.2	7.0	2.6
5-CH_3-$H_4PteGlu_{5-6}$	28−42	0.5−0.8	5−8	0.1−0.15	1.5	0.08	0.6	0.03
total folate	62	1.1−1.6	63.0	1.2−1.6	10.7	2.3	28	2.6

(B) Tissue Concentrations of Formyl Tetrahydrofolates

	mouse liver[f]				L1210[g]			
	cytosol [μM]	K_i's[h]	mitochondria [μM]	K_i's[h]	cytosol [μM]	K_i's[h]	mitochondria [μM]	K_i's[h]
10-CHO−$H_4PteGlu_{5-6}$	11.7	4.8	21	8.8			5.6	2.4
5-CHO−$H_4PteGlu_{5-6}$	5.4	0.064	7.2	0.085	0.5	0.008	5.6	0.08
total formyl folate	17	4.9	28	8.9	0.5	0.008	11.2	2.5

[a] A value for mouse liver total folates of 38 nmol/g wet weight was obtained from Dr. David Priest (*44*, personal communication). A distribution of 66% of total folate contained within the cytosolic and 33% of total folate within mitochondrial compartments of the rat liver was taken from ref *37*. Concentrations of total folate contained within each compartment were calculated based on estimated cytosolic and mitochondrial compartmental volumes from stereological analysis of electron micrographs of rat liver hepatocytes (*45*). [b] The mean (5 pmol/10^6 cells) of values of total folate from references (*5*, *33*, *46*) was used to estimate folate cofactor concentrations assuming: 10^9 L1210 cells = 0.67 mL intracellular water and L1210 cytosol and mitochondria contain 80 and 20% of total cellular folates, respectively (*38*). Nuclear, mitochondrial, and rough endoplasmic reticulum volumes were assumed to be 38, 5, and 0.7% of total L1210 cell volume, respectively, as determined previously by morphometric data calculated from electron micrographs of L1210 cells (*47*). Smooth endoplasmic reticulum, lysosomes, and golgi compartments each comprised less than 0.4% of the total cell volume in human T-cell ALL (*48*) and thus were not included in the calculation of L1210 cytosolic compartment. [c] Values for $H_4PteGlu$/5,10-CH_2-$H_4PteGlu_{5-6}$, and 5-CH_3-$H_4PteGlu_{5-6}$ represent a concentration range calculated based on cofactor distributions (%) within the cytosol and mitochondria of liver tissue from refs *37* and *41*. [d] Values for the $H_4PteGlu_{5-6}$/5,10-CH_2-$H_4PteGlu_{5-6}$ pool in L1210 cells were estimated based on cellular distributions taken from ref *38*. Values for 5-CH_3-$H_4PteGlu_{5-6}$ were estimated based on the total amount of the derivative in L1210 cells (*5*) and assuming 5-CH_3-$H_4PteGlu$ comprises 2% of the mitochondrial folate pool (*38*). [e] The amount of inhibition (K_i's) contributed by each cofactor was estimated using values for $K_{i\ slope}$ from Table 2. The average of the individual K_i values for $H_4PteGlu_5$ and 5,10-CH_2-$H_4PteGlu_5$ were used to calculate the amount of feedback inhibition contributed by the $H_4PteGlu_{5-6}$ /5,10-CH_2-$H_4PteGlu_{5-6}$ pool. [f] Values for 10-CHO-$H_4PteGlu_{5-6}$ and 5-CHO-$H_4PteGlu_{5-6}$ pools in hepatocytes were estimated based on cellular distributions taken from ref *41* and values for total folate presented in Table 3A. [g] Values for 10-CHO-$H_4PteGlu_{5-6}$ and 5-CHO-$H_4PteGlu_{5-6}$ pools in L1210 cells were estimated based on cellular distributions taken from ref *38* and values for total folate presented in Table 3A. [h] The amount of inhibition (K_i's) contributed by each cofactor was estimated using values for $K_{i\ slope}$ from Table 2.

preliminary report indicated that deletion of the first eight amino acids of human FPGS inactivated the enzyme and that, of a series of mutations made in this peptide, modification of Tyr-3 had the largest effect on enzyme activity (*36*). The structure of the *L. casei* FPGS indicates that the Ω loop partially wraps around Tyr-3 (*12*). Likewise, unpublished experiments from our laboratory demonstrated that deletion of the first four amino acids in human cytosolic FPGS resulted in a 60−80% decrease in k_{cat} with different substrates. Thus, the N-terminal peptide influences the catalytic activity of mammalian FPGS, apparently by influencing the three-dimensional structure of the active site.

The literature allows some estimates to be made of the concentration of folate cofactors in mouse liver and L1210 cells. However, the most meaningful estimates must take into account the known fact that cellular folates are distributed between the cytosolic and mitochondrial compartments. Mitochondria have been estimated to contain 20−30% (*37*, *38*) and, in some cases, as much as 50% (*39*) of the total cellular folate cofactor pool. In both mouse liver and L1210 cells, two sets of FPGS mRNAs are expressed, one of which translates to cytosolic FPGS, and the other adds a leader sequence to the cytosolic FPGS, allowing penetration of enzyme to the mitochondrial matrix (*11*). Experience with other mitochondrial enzymes (*40*) predicts that the FPGS mitochondrial leader sequence would be cleaved shortly after entry of enzyme into the mitochondrial matrix. As a first estimate, we assume that the sensitivity of the mitochondrial FPGS in mouse liver and L1210 cells to feedback is about that seen with the cytosolic FPGS species in each of these tissues. Previous work indicated that 5-CH_3-$H_4PteGlu_n$ and 10-CHO-$H_4PteGlu_n$ are not evenly distributed between cytosolic and mitochondrial compartments. In rat liver, the majority of 5-CH_3-$H_4PteGlu_n$ was reported to be in the cytosol (*37*, *41*), which would agree with the distribution of 5,10-methylenetetrahydrofolate reductase and methionine synthase in the cytosol. Others have reported that most of the 10-CHO-$H_4PteGlu_n$ in rat liver is localized in the mitochondria (*42*). However, it seems likely that both mitochondrial and cytosolic fractions contain appreciable concentrations of 10-CHO-$H_4PteGlu_n$, in at least some cell types, in keeping with the need for this cofactor for purine synthesis in the cytosol/nuclei and for the production of formate in the mitochondria for export to the cytosol (*43*).

The concentration of folate cofactors in mouse hepatocytes is substantially higher than that in L1210 cells (Table 3A), in accord with the lower sensitivity of mouse liver FPGS to feedback inhibition by tetrahydrofolate polyglutamates as compared with L1210 FPGS. Hepatocyte cytosol is reported to have ≈6-fold higher concentration of total folates than cytosol of L1210 cells and mitochondrial folate concentrations were ≈2-fold higher in hepatocytes than in L1210 cells (Table 3A). If the kinetics of feedback by $H_4PteGlu_5$ and 5-CH_3-$H_4PteGlu_5$ on FPGS in mouse liver and L1210 subcellular compartments are compared, the substantially higher concentrations of these cofactors in mouse liver are matched by the difference in sensitivity of the two FPGS species to feedback. That is, the difference between these two FPGS species would allow accumulation of higher levels of $H_4PteGlu_5$ and 5-CH_3-$H_4PteGlu_5$ before feedback began

to limit the pathway. The literature describing distribution of individual folate cofactors in L1210 cells and hepatocytes allowed estimation of $H_4PteGlu_{5-6}$ and 5-CH_3-$H_4PteGlu_{5-6}$ concentrations in the mitochondria and cytosols of these cells. A more difficult assessment of in situ feedback control is faced when one relates pool sizes of 10-CHO-$H_4PteGlu_{5-6}$ to the feedback inhibition affected by these pools. Interconversion of 10-CHO- and 5-CHO-$H_4PteGlu_n$ during sample tissue preparation and/or chromatography makes estimation of the 10-CHO-$H_4PteGlu_{5-6}$ cofactor pool in cells and subcellular fractions particularly challenging, and the literature values for 10-CHO-$H_4PteGlu_n$ are difficult to place into perspective (Table 3B). However, the conclusion can be drawn that 10-CHO-$H_4PteGlu_{5-6}$ could possibly exert substantial feedback regulation of L1210 and mouse liver FPGS and may play an important, and probably the dominant, role in determining the activity of mouse liver mitochondrial FPGS. Overall, it would appear that the total folate cofactor concentrations found in mouse hepatocytes and proliferating L1210 cells are different as a result of the difference in the ability of long chain folylpolyglutamates to exert feedback inhibition upon the species of FPGS expressed in that tissue.

The above discussion assumes that all tetrahydrofolylpolyglutamate cofactors are freely diffusible within cytosolic solvent phase on the one hand and mitochondrial matrix solvent on the other. However, the intracellular protein binding capacity for folates is substantial, especially in hepatic tissue. The amounts of SHMT and C1-tetrahydrofolate synthase are the equivalent of a concentration of 25 μM in folate binding sites (*6*). 10-Formyltetrahydrofolate dehydrogenase, which has been shown to exhibit tight binding of $H_4PteGlu$, contributes an estimated 14 μM in H_4-PteGlu binding sites in mouse liver (*49*). The folate content of L1210 cells has been shown to behave as macromolecules unless strong denaturing conditions are used during extraction (*50*), a result that constitutes very direct evidence that the majority of tetrahydrofolate cofactors are bound to cellular proteins in vivo. However, the simple fact remains that folylpolyglutamate cofactors are found within tissues as long chain (Glu_5 or higher) polyglutamates and therefore must be accessible to FPGS. Hence, either protein-bound folates are still accessible to the active site of FPGS, or the rate of exchange of polyglutamate folates with solvent phase is rapid compared with the rate of binding of folates to FPGS.

ACKNOWLEDGMENT

We thank Dr. Clyde Smith of the University of Auckland, New Zealand, for generously making available the coordinates of a crystal structure of the *L. casei* FPGS bound to 5,10-methylenetetrahydrofolate prior to publication, Dr. David Priest of the Medical University of South Carolina for converting the data of reference (*44*) to a form that allowed the comparisons in Table 3A, and Dr. Chuan Shih of Eli Lilly Company for samples of synthetically prepared DDATHF polyglutamates. We also are indebted to Dr. Verne Schirch for some very helpful discussions about this work and for his critical analysis of the manuscript.

REFERENCES

1. Blakley, R. L. (1957) *Biochem. J. 65*, 331−342.
2. Baugh, C. M., and Krumdiek, C. L. (1971) *Ann. N. Y. Acad. Sci. 186*, 7−28.
3. Blakley, R. L., and Benkovic S. J. (1984) *Folates and Pterins: Volume 1, Chemistry and Biochemistry of Folates.* John Wiley & Sons, Inc., New York.
4. Priest, D. G., Happel, K. K., Magnum, M., Bednarek, J. M., Doig, M. T., and Baugh, C. M. (1981) *Anal. Biochem. 115*, 163−169.
5. Moran, R. G., Werkheiser, W. C., and Zakrzewski, S. F. (1976) *J. Biol. Chem. 251*, 3569−3575.
6. Schirch, V., and Strong, W. B. (1989) *Arch. Biochem. Biophys. 269*, 371−380.
7. Taylor, R. T., and Hanna, M. L. (1977) *Arch. Biochem. Biophys. 181*, 331−344.
8. Shane, B. (1989) *Vitam. Horm. 45*, 263−335.
9. McBurney, M. W., and Whitmore, G. F. (1974) *Cell. 2*, 173−182.
10. Roy, K., Mitsugi, K, and Sirotnak, F. M. (1997) *J. Biol. Chem. 272*, 5587−5593.
11. Turner, F. B., Andreassi, J. L., II, Ferguson, J., Titus, S., Tse, A., Taylor, S. M., and Moran, R. G. (1999) *Cancer Res. 59*, 6074−6079.
12. Sun, X., Bognar, A. L., Baker, E. N., and Smith, C. A. (1998) *Proc. Natl. Acad. Sci. U.S.A. 95*, 6647−6652.
13. Sheng, Y., Sun, X., Shen, Y., Bognar, A. L., Baker, E. N., and Smith, C. A. (2000) *J. Mol. Biol. 302*, 427−440.
14. Sun, X., Cross, J. A., Bognar, A. L., Baker, E. N., and Smith, C. A. (2001) *J. Mol. Biol. 310*, 1067−1078.
15. Stover, P., and Schirch, V. (1992) *Anal. Biochem. 202*, 82−88.
16. Huennekens, F. M., Matthews, C. K., and Scrimgeour, K. G. (1963) *Methods Enzymol. 6*, 802−806.
17. Blakley, R. L. (1969) *The Biochemistry of Folic Acid and Related Pteridines*, John Wiley & Sons, Inc., New York.
18. Futterman, S. (1957) *J. Biol. Chem. 228*, 1031−1038.
19. Coward, J. K., Parameswaran, K. N., Cashmore, A. R., and Bertino, J. R. (1974) *Biochemistry 13*, 3899−3903.
20. Blakley, R. L. (1960) *Nature 188*, 231−232.
21. Bertino, J. R., Perkins, J. P., and Johns, D. G. (1965) *Biochemistry 4*, 839−846.
22. Sakami, W., and Ukstins, I. (1961) *J. Biol. Chem. 236*, PC 50.
23. Moran, R. G., and Colman, P. D. (1982) *Anal. Biochem. 122*, 70−78.
24. Sanghani, P. C., and Moran, R. G. (2000) *Protein Expr. Purif. 18*, 36−45.
25. Bradford, M. M. (1976) *Anal. Biochem. 72*, 248−254.
26. Moran, R. G., and Colman, P. D. (1984) *Anal. Biochem. 140*, 326−342.
27. Cleland, W. W. (1979) *Methods Enzymol. 63*, 103−138.
28. Sanghani, S. P., Sanghani, P. C., and Moran, R. G. (1999) *J. Biol. Chem. 274*, 27018−27027.
29. Chen, L., Qi, H., Korenberg, J., Garrow, T. A., Choi, Y. J., and Shane, B. (1996) *J. Biol. Chem. 271*, 13077−13087.
30. Moran, R. G., and Colman, P. D. (1984) *Biochemistry 23*, 4580−4589.
31. Fromm, H. J. (1975) *Mol. Biol. Biochem. Biophys. 22*, 41−160.
32. Cichowicz, D. J., and Shane, B. (1987) *Biochemistry 26*, 513−521.
33. Tse, A., and Moran, R. G. (1998) *J. Biol. Chem. 273*, 25944−25952.
34. McGuire, J. J., Hsieh, P., Coward, J. K., and Bertino, J. R. (1980) *J. Biol. Chem. 255*, 5776−5788.
35. Cook, J. D., Cichowicz, D. J., George, S., Lawler, A., and Shane, B. (1987) *Biochemistry 26*, 530−539.
36. Qi, H., Atkinson, I., Xiao, S., Choi, Y., Tobimatsu, T., and Shane, B. (1999) *Adv. Enz. Regul. 39*, 263−273.
37. Carl, G. F., Hudson, F. Z., and McGuire, B. S., Jr. (1995) *J. Nutr. 125*, 2096−2103.
38. Trent, D. F., Seither, R. L., and Goldman, I. D. (1991) *Biochem. Pharmacol. 42*, 1015−1019.
39. Lin, B., Haung, R., and Shane, B. (1993) *J. Biol. Chem. 268*, 21674−21679.
40. Akio, I. (1999). *Biochem. Biophys. Res. Commun. 265*, 611−616.

41. Horne, D. W., Patterson, D., and Cook, R. J. (1989) *Arch. Biochem. Biophys. 270*, 729−733.
42. Shane, B. (1995) in *Folate in Health and Disease* (Bailey, L. B., Ed.) pp 1−22, Marcel Decker, Inc., New York.
43. Appling, D. R. (1991) *FASEB J. 5*, 2465−2650.
44. Schmitz, J. C., Grindey, G. B., Schultz, R. M., and Priest, D. G. (1994) *Biochem. Pharmacol. 48*, 319−325.
45. Weibel, E. R., Staubli, W., Gnagi, H. R., and Hess, F. A. (1969) *J. Cell. Biol. 42*, 68−91.
46. Priest, D. G., Bunni, M., and Sirotnak, F. M. (1989) *Cancer Res. 49*, 4204−4209.
47. Fenczyn, J., Kawiak, J., and Kilarski, W. (1979) *Folia. Histochem. Cytochem. 17*, 335−344.
48. Kujawa, M., Baranska, W., Ochocka, M., Slubowski, T., and Baran, W. (1983) *Acta Haematol. Pol. 14*, 1−11.
49. Kim, D. W., Huang, T., Schirch, D., and Schirch, V. (1996) *Biochemistry 35*, 15772−15783.
50. Matherly, L. H., and Muench, S. P. (1990) *Biochem. Pharm. 39*, 2005−2014.

BI015644D